

BEAM DYNAMICS FOR INTENSE L-BAND ELECTRON LINAC*

S. H. Kim[#], B. Park, S. I. Moon, J. S. Oh, M. H. Cho and W. Namkung

POSTECH, Pohang 790-784, Korea

Abstract

We are now developing an intense L-band electron linac with a traveling-wave accelerating structure for irradiation applications. It is capable to produce 10 MeV electron beams of 30 kW by a pulsed klystron of 25 MW with a 60 kW average power. Bunching and accelerating cavities operated with $2\pi/3$ mode at 1.3 GHz are designed by the SUPERFISH code. Focusing solenoids are designed by the POISSON code. Using electromagnetic field configurations obtained by these codes, a simulational study on the beam dynamics is conducted by the PARMELA code. As results, the beam envelope supports a transmission efficiency over 91% with the E-gun current of 1.6 A.

INTRODUCTION

For industrial irradiation applications, in general, the electron beam energy is limited by 10 MeV due mainly to neutron production. One needs higher currents for high power beams. With increased beam currents, the beam loading effect comes into play in reducing the beam energy. In the past, there were a few RF linacs built in the range of 25-30 kW [1]. In order to obtain 30 kW beams with a single klystron and the vertical arrangement of accelerator beamlines, we are developing an intense L-band linac with a 25-MW pulsed klystron. In the development of the L-band electron linac, simulation studies are conducted; the SUPERFISH code for RF cavity design [2], the POISSON code for the magnetic field design [3], and the PARMELA code for beam dynamics [4]. This paper presents results of beam dynamics for a 30-kW RF linac.

BEAMLINER

The accelerator beamline consists of E-gun, pre-buncher, gate valve, accelerating column with focusing solenoids, and beam scanner. The E-gun is a diode type one powered by a 6- μ s, 80-kV modulator. The beam is bunched by the modulating voltage in the pre-buncher. The pre-bunched beam is injected to the accelerating column, which is consisted of the bunching section and the normal accelerating section. The RF power of pulsed 25 MW is introduced into the first cavity of the bunching section, and RF wave travels through all the cavities, and it is drained from the last cavity into a matched load. At the end of the accelerating column, the electron beam is accelerated up to 10 MeV with the input beam current of

1.6 A. This beam enters into a beam scanner. The accelerator is mounted vertically and the beam scanner sweeps beams horizontally.

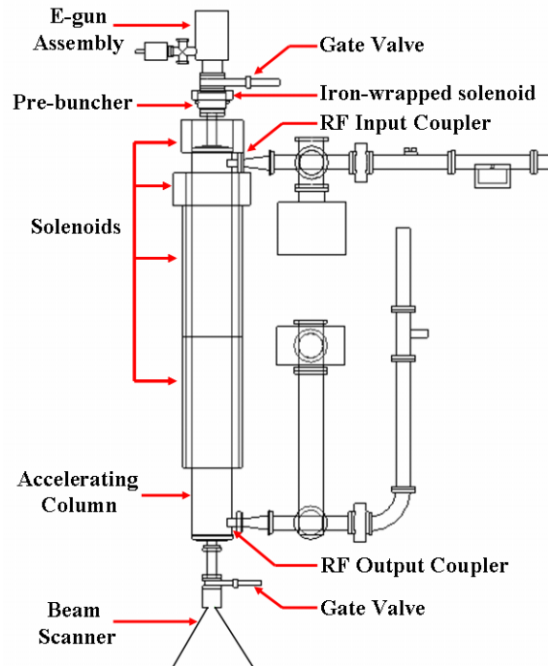


Figure 1: Drawing of the L-band electron accelerator.

Pre-buncher

The pre-buncher is a re-entrant cavity with a standing-wave resonant frequency of 1.3 GHz. The material of the cavity is stainless steel for a lower quality factor and the beam loading effect. The velocity modulation by the pre-buncher contains 62% of electron beams within a phase-angle interval of 78° at the entrance of the accelerating column.

Accelerating Column

The accelerating column is a disk-loaded waveguide. It has the bunching section of 5 cavities and the normal accelerating section of 26 cavities. The attenuation coefficient of each cavity is shown in Table 1. The bunching cavities have smaller values than the normal cavity since low electric fields in the bunching section guarantee a higher capture rate [5]. Table 1 also shows the phase velocity in each cavity for effective bunching.

*Work supported by KAPRA and PAL
[#]khan777@postech.ac.kr

Table 1: Phase velocity and attenuation coefficient

Cavity	Phase velocity / Speed of light	Attenuation Coefficient (Nep/m)
1 st buncher	0.65	0.0538
2 nd buncher	0.75	0.0489
3 rd buncher	0.88	0.0442
4 th buncher	0.92	0.0431
5 th buncher	0.98	0.0415
Normal	1.00	0.0623

The normal accelerating section is a constant-impedance structure. The shunt impedance is 44.0 MΩ/m, and the quality factor is 2.1×10^4 . Every cavity is operated with the $2\pi/3$ mode at the resonant frequency of 1.3 GHz. For simulations with the SUPERFISH code, we used two eigen-modes; one is a cosine-function boundary condition and another is a sine-function boundary condition.

Since the RF power attenuates as passing through the accelerating column, the longitudinal electric field is expressed as [6]

$$E(z) = E_0 \exp(-\alpha z) \sin \phi - I r_s (1 - \exp(-\alpha z)), \quad (1)$$

where r_s is the shunt impedance, $E_0 = \sqrt{2\alpha P_0 r_s}$, α is the attenuation coefficient listed in Table 1, P_0 is the input power from the RF source, and ϕ is the phase of the accelerating field. The last term represents the beam loading effect. The actual longitudinal electric field is shown in Figure 2 at an arbitrary initial phase. Since the electric field at the last cavity is almost zero, this accelerator is operated in the fully beam-loaded condition.

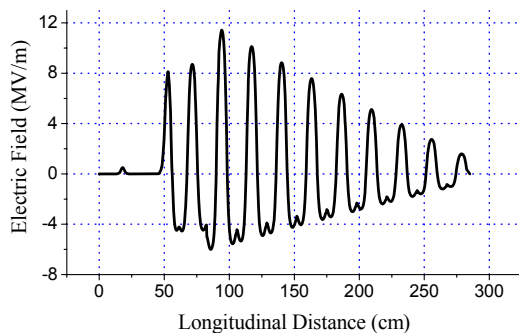


Figure 2: Longitudinal electric fields.

Focusing Solenoids

There are five solenoid magnets, and the focusing magnetic field is shown in Figure 3. The location of the V-shaped valley corresponds to the input coupler. The accelerating column ends at 298 cm.

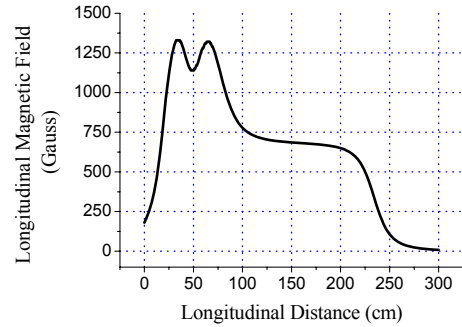


Figure 3: Longitudinal magnetic fields.

BEAM DYNAMICS

Beam Energy and Beam Envelope

The beam energy is obtained by the PARMELA simulation, and the axial energy distribution is shown in Figure 4. The energy gain of the electron beam is gradually reduced as the beam passes through the accelerating column, corresponding to the longitudinal electric field in Figure 2.

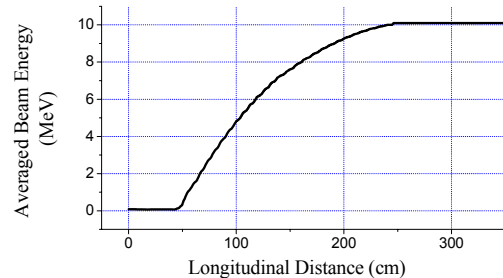


Figure 4: Beam energy.

The beam envelope is shown in Figure 5. With the magnetic fields in Figure 3, the electron beam is focused sufficiently small in the acceleration column, and it is slightly expanded for a convenient size in use of scanning at the target.

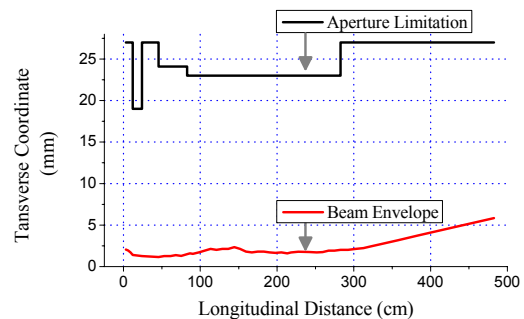


Figure 5: Beam envelope.

Beam Characteristics

As the result of the PARMELA simulations, the phase and energy spectra are shown in Figure 6 and 7, respectively. At the exit of the E-gun, the electron beam is long enough for an RF period in Figure 6(a), and the beam is bunched in the phase angle as shown in Figure 6(b). The mono-energy beam from the E-gun gains energy through the acceleration to have an energy-spread at the end of the accelerating column shown in Figure 7 (a) and (b).

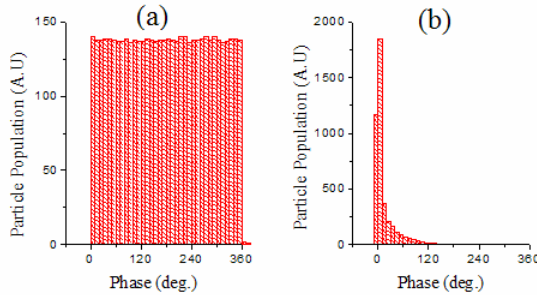


Figure 6: Phase spectrum (a) Exit of E-gun, (b) Exit of accelerating column.

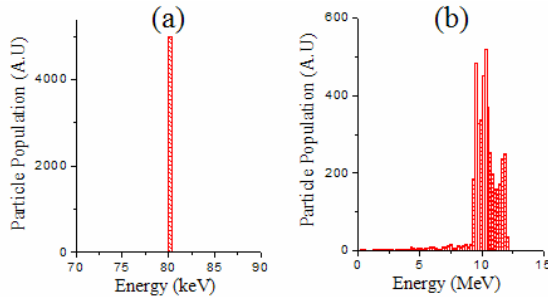


Figure 7: Energy spectrum (a) Exit of E-gun, (b) Exit of accelerating column.

Dependency on Operating Conditions

To achieve the beam energy of 10 MeV and the averaged beam power of 30 kW with a duty factor of 2.1×10^{-3} , input parameters are optimized for the E-gun current and the RF power. By simulations with various values of input beam current and RF power, contour maps are constructed as shown in Figure 8 and 9.

As the input beam current increases the output beam energy becomes lower due to the beam loading effect in Figure 8. The output beam power increases at first, but it decreases after an optimum value of the input current in Figure 9. From these contour maps, the nominal operating conditions are determined as the input beam current of 1.6 A, and the input RF power of 25 MW.

SUMMARY

Beam dynamics is investigated for an intense L-band travelling-wave linac under development at PAL and KAPRA. The beam current is high enough to be operated under the fully beam-loaded condition. From the simulation results, we confirmed that the beam envelope

is small enough for the safe beam transmission. Also, the phase and energy spreads are acceptable for its use in irradiation applications. By adjusting the input RF power and the E-gun current, we obtained the optimum conditions for the 10 MeV, 30 kW averaged beams.

ACKNOWLEDGEMENT

The authors are very grateful to Dr. Luo Yingxiong at IHEP, Beijing for his helpful discussion on general issues of the accelerator system and the design of the accelerating structure.

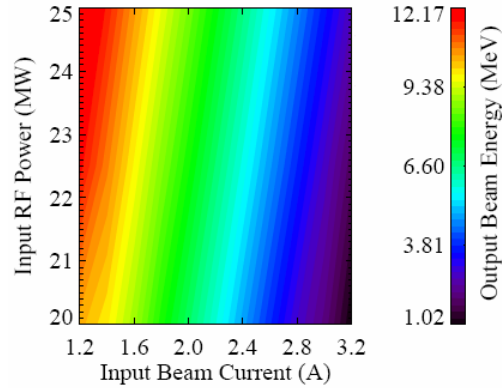


Figure 8: Output beam energy with input beam current and RF power.

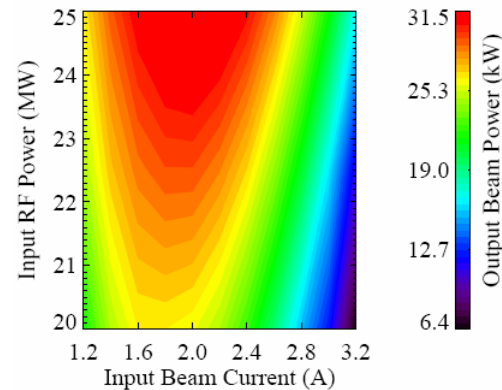


Figure 9: Output beam power with input beam current and RF power.

REFERENCES

- [1] Y. Kamio, "10 MeV 25 kW Industrial Electron Linacs," in *Proc. Int. Linac Conf.* (Geneva, Switzerland, Aug. 26-30 1996), 836 (1996).
- [2] SUPERFISH is a trademark of LANL.
- [3] POISSON is a trademark of LANL.
- [4] PARMELA is a trademark of LANL.
- [5] M. Chodorow, E. L. Ginzton, W. W. Hansen, R. L. Kyhl, R. B. Neal, and W. K. H. Panofsky, *Rev. Sci. Inst.* **26**, 2 (1955).
- [6] Y. Thiery, J. Gao, and J. Le Duff, "Design Studies for a High Current Bunching System for CLIC Test Facility (CTF3) Drive Beam," in *Proc. Int. Linac Conf.* (Monterey, CA, Aug. 21-25, 2000), 95 (2000).